Mon. Not. R. Astron. Soc. **271**, 75–80 (1994)

Secondary calibrators at submillimetre wavelengths

Göran Sandell★
Joint Astronomy Centre, 660 N. A'ohōkū Place, Hilo, HI 96720, USA

Accepted 1994 June 8. Received 1994 February 7

ABSTRACT

This paper is the first attempt to establish a set of secondary calibrators for submillimetre continuum photometry. In total we include photometry on 21 sources (ultracompact H II regions, compact bipolar outflow sources and protoplanetaries). These sources are all calibrated relative to Mars and Uranus, which are the primary submillimetre standards. Data are given for all the major atmospheric windows in the (sub)millimetre regime for a standard set of broad-band filters used in the common-user bolometer UKT14, i.e. 2, 1.3 and 1.1 mm, and 800, 450 and 350 μm. For most sources, some data are also given for the two narrow-band filters at 850 and 750 μm, which split up the 800-μm window. For some sources we have about 20 independent observations spread over a period of about 2 years. The standard deviations of the data show that we typically achieve an accuracy of a few per cent at 1 mm, and about 10–15 per cent at 450 and 350 μm. The errors do not include the uncertainties in the absolute flux densities of the planets, which add an additional 5–10 per cent in total errors.

Although these calibrators are mainly intended for use on the James Clerk Maxwell Telescope (JCMT), the list should also be applicable to other telescopes. At JCMT, the present calibrator set has already been in use for about 2 years.

Key words: techniques: photometric – ISM: general – radio continuum: general.

1 INTRODUCTION

The new generation of large millimetre and submillimetre telescopes (JCMT, CSO, IRAM and SEST), located at moderate to good submillimetre sites, has significantly increased the number of submillimetre continuum observations which previously were obtained mainly on large optical telescopes. At the same time, it has become painfully clear that more than just planets are needed to calibrate such observations. The half-power beamwidths (HPBWs) of these antennas are either too small or not clean enough to enable a reliable derivation of the beam coupling to large planets which may also cover the first sidelobes of the beam. This is always the case for Jupiter, but even Mars and Venus can at times be too large. Furthermore, telescopes like the JCMT have most observing runs scheduled in 8-h shifts, during which time there may be no planets available. In addition, submillimetre photometry is notoriously difficult: the atmospheric windows are at most semi-transparent and the transparency is a strong function of the precipitable water vapour (PWV). The submillimetre sky is hardly ever photometric in the sense to which one is accustomed in the optical or near-IR.

At JCMT we started early to establish secondary standards for submillimetre continuum photometry. A first-draft catalogue was released in 1989 (Sandell 1989). Since then, observers have been provided with updates on an individual basis, and from 1991 December the present catalogue has been available to JCMT observers. The catalogue has also been used to some extent at the Caltech Submillimeter Observatory (CSO).

2 SOURCE SELECTION

An ideal calibration source should be bright, compact and non-variable. Unfortunately, such sources do not exist. The best choice is to use planets like Mars, Venus, Uranus and Neptune. Both Mars and Venus are too extended for a telescope like JCMT when the planets are close to perihelion. Nevertheless, Mars is the absolute calibrator for all submillimetre observations, and all other planets are calibrated relative to Mars (see e.g. Griffin et al. 1986; Orton et al. 1986), despite the fact that, at short wavelengths, the brightness temperature of Mars follows the diurnal tempera-

★E-mail: SANDELL@JACH.HAWII.EDU.

ture variation across the disc, which varies by more than 20 per cent (Kieffer et al. 1977). The diurnal variation of the disc-averaged temperature actually changes sign somewhere between 3.3 mm and 20 μm, and is probably quite small in the submillimetre (see e.g. Griffin et al. 1986), but the brightness temperature of Mars may also be affected by seasonal variations and possible effects of dust storms. Additionally, Saturn should be excluded, because the rings contribute to the total submillimetre flux density, which is also dependent on their inclination. Jupiter is a frequently used calibrator, but, on a telescope like JCMT, it is impractical because its disc covers the JCMT beam up to the first-sidelobe level. In this case the coupling to the beam is almost impossible to estimate. Neptune is fainter than Uranus and in the same area of the sky for the next few decades. This means that there is no advantage in observing it, unless one needs a small-diameter source. Venus, which at times could be useful, does not yet have brightness temperatures that are determined accurately enough in the submillimetre regime, and therefore the only two planets that are commonly used as calibrators on JCMT are Mars and Uranus. All other sources have been calibrated against these two planets.

Apart from planets, the strongest known sources in the submillimetre regime are ultracompact H II regions (UCHII regions), which radiate most of their energy in the far-infrared. These are constant, i.e. non-variable, but they often occur in groups and are almost always associated with extended emission. The youngest stars in this group, i.e. massive protostars like IRc2 in OMC-1, lie in regions with significant extended emission, and furthermore these stars are seldom isolated, which causes additional confusion. Although OMC-1 IRc2 was originally in the calibrator list, it was found that large chop-throws were required (typically 150 arcsec), and it was often not possible to peak up reliably on the source because of confusing emission from the northern ridge sources (Wright et al. 1992). At 450 and 350 μm, photometry of IRc2 also appears to be much more sensitive to the shape of the error beam. The derived flux densities show a large scatter over time, which one would expect if the error pattern were not symmetric and the contribution from the error beam were significant. We have therefore decided not to use OMC-1 IRc2 as a secondary calibrator. It is, however, possible to find isolated UCHII regions that are point-like with source sizes of ~10 arcsec. The majority of the secondary calibrators come from this group. At 450 μm, high-resolution mapping has shown that most UCHII regions have fainter secondary components, i.e. occur in small tight clusters, and one should avoid trying to use them as calibrators with HPBWs of ≤10 arcsec. A few have strong free–free emission, and are therefore useful as calibrators longward of 1 mm. The majority, however, are faint in the free–free regime. We have included a few UCHII regions that are not ideal because they have nearby bright sources and are surrounded by extended lumpy emission. Additional work may show that these sources must be eliminated.

Another group of sources are the low-luminosity protostars, which are cold and extremely rich in dust. Only a few, however, are sufficiently bright and isolated to serve as calibrators. Like the UCHII regions, they are always surrounded by fainter extended dust emission.

The last group of sources that are potential secondary calibrators are the asymptotic giant branch (AGB) stars, i.e. stars in their late stellar evolutionary stage, which are surrounded by large dust-rich envelopes. Most AGB stars are faint submillimetre emitters, however, and may furthermore be variable (Knapp, Sandell & Robson 1993). The stars included here are protoplanetary nebulae, or young planetaries that are strong enough to serve as calibrators, or long-period variables like VY CMa and CW Leo (IRC + 10216). IRC + 10216 is, however, strongly variable in the (sub)millimetre (Fig. 1, Knapp et al., in preparation). Even so, we have retained it as a secondary calibrator for two reasons: (i) the variations are periodic with a well-defined light curve (Fig. 1); and (ii) it is located in a region of the sky where we have no other flux calibrators. If IRC + 10216 were not used, one would instead have to use strong blazars like 3C 273 or 3C 279 to boot-strap the calibration to a planet or a protostar on either side of the Galactic plane (e.g. NGC 2071IR or 16293 − 2422). Blazars, however, are always too faint to serve as calibrators at 450 and 350 μm, and hence the only adequate source appears to be IRC + 10216, unless we can find another standard. We have occasionally used TW Hya, a T Tauri star (Weintraub, Sandell & Duncan 1989), but this object is even fainter than IRC + 10216.

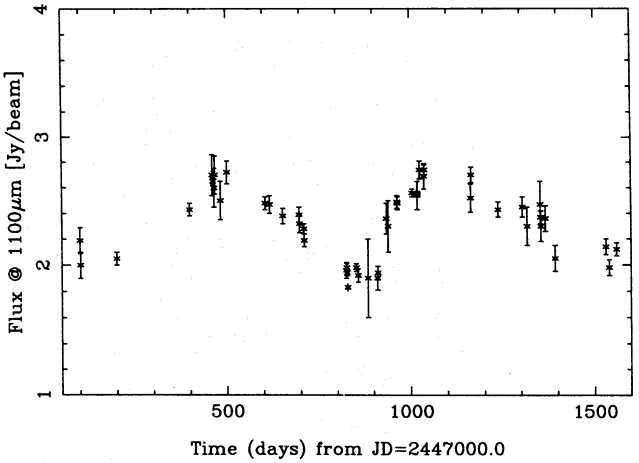

Figure 1. The 1.1-mm 'light curve' of the long-period variable IRC + 10216, observed over two cycles.

Table 1 gives the adopted positions for each source in our secondary calibrator list, together with the deduced source size, which in most cases is determined from fully sampled 800-μm maps. Of the AGB stars, only NGC 7027 and IRC + 10216 have been mapped with JCMT, and all the others are claimed to appear point-like, i.e. to have sizes ≤5 arcsec based on numerous five-point maps and aperture photometry at 800 μm. This does not mean that all the emission comes from a point source; it simply means that the emission is dominated by the unresolved core of the dust emission (see e.g. Knapp et al. 1993).

3 OBSERVATIONS AND DATA REDUCTION

The data for Table 2 have been obtained with the JCMT during the period 1989 September to 1991 November, with a few data points added from observations obtained later. The starting point for the basic data set, 1989 September, is rather arbitrary. At that time we made a major effort to improve the surface accuracy of the telescope, achieving an rms ≤30 μm. However, for some data, taken toward the end of the period (summer and autumn 1991) when the surface had deteriorated, the submillimetre performance was poor.

Table 1. Coordinates and sizes of secondary calibrators.

SOURCE	$\alpha \times \delta$ (″)	R.A.(1950) h m s	DEC.(1950) ° ′ ″
W3(OH)	14.2 × 10.2	02 23 16.45	+ 61 38 57.2
G343.0	10.0 × 14.8	16 54 43.77	− 42 47 32.4
NGC 6334I	12.2 × 6.2	17 17 32.34	− 35 44 03.1
G5.89	9.0 × 10.3	17 57 26.75	− 24 03 56.0
G10.62	11.8 × 10.1	18 07 30.66	− 19 56 29.1
G34.3	6.2 × 7.8	18 50 46.17	+ 01 11 12.6
G45.1	9.4 × 10.0	19 11 00.42	+ 10 45 42.9
K3-50	10.6 × 5.5	19 59 50.09	+ 33 24 19.4
ON-1	11.3 × 16.6	20 08 09.91	+ 31 22 42.3
W75N	8.5 × 10.9	20 36 50.00	+ 42 26 58.0
NGC 7538IRS1	20.4 × 17.6	23 11 36.62	+ 61 11 49.6
GL 490	< 5 × 8.7	03 23 39.22	+ 58 36 35.6
L1551-IRS5	5.2 × 10	04 28 40.24	+ 18 01 42.1
NGC 2071IR	10.7 × 13.0	05 44 30.7	+ 00 20 45.0
16293-2422	9.0 × 10.6	16 29 21.05	− 24 22 15.5
CRL 618	< 5	04 39 34.	+ 36 01 16.0
VYCMa	< 5	07 20 54.7	− 25 40 12.4
OH231.8	< 5	07 39 59.0	− 14 35 41.0
IRC+10216	9.2 × 10.8	09 45 14.89	+ 13 30 40.8
CRL 2688	< 5	21 00 19.9	+ 36 29 45.0
NGC 7027	~ 10	21 05 09.4	+ 42 02 03.0

Comparison with earlier JCMT data given by Sandell (1989) shows that the change in surface accuracy did not significantly change the characteristics of the telescope (except for sources like OMC-1 IRc2), and the flux densities for the secondary calibrators given in this paper obtained over the lifetime of the JCMT are rather constant. The main effect of a poor surface is that it can result in the telescope gain and HPBW becoming functions of elevation. As long as the sources are effectively point-like, the main outcome is poorer photometry because changes in the telescope gain cannot be separated from changes in atmospheric opacities.

All observations were made using the common-user bolometer UKT14 at the Nasmyth focus on JCMT. The main characteristics of UKT14 were described by Duncan et al. (1990) and we will only summarize the main features here. UKT14 is a sensitive, ^{3}He-cooled, single-channel bolometer with filters that cover all major submillimetre windows. It has a variable iris which permits diffraction-limited observations at 1.1 mm, and 850, 800, 750, 600, 450 and 350 μm. For a fully open aperture, i.e. 65 mm, the HPBW is approximately constant and about 18.5 arcsec at all filters, although there is some frequency dependence. At 2.0 and 1.3 mm the optics overilluminate the primary, giving HPBWs of ~19.5 arcsec at 1.3 mm and ~27.5 arcsec at 2 mm. Sky cancellation is achieved with a chopping secondary and by nodding the telescope, following the normal convention. The default chop is 60 arcsec in azimuth with a chop frequency of 7.8125 Hz, although chop throws up to 150 arcsec are used frequently.

Planetary fluxes for each filter, computed using the JCMT utility program FLUXES, were originally based on the planetary brightness temperatures by Griffin et al. (1986) and Orton et al. (1986). The FLUXES program was updated in 1992 August to take into account the revised Uranus temperatures of Griffin & Orton (1993), but since the differences to earlier data are minor, this change is not expected to affect the quality of the data given in Table 2. We also note that the 850-μm filter in UKT14 was changed in 1992 April. The main consequence of the new filter is in the improved noise performance; the 850-μm data in Table 2 should still be valid.

All potential calibrators are normally very bright, and the statistical photometric error is never a limiting factor, except at the longest wavelengths. A rule of thumb is to try to achieve a signal-to-noise ratio of ~50 to enable accurate determination of the extinction throughout the night. The extinction correction is always the dominant error, especially at short wavelengths, where the transmission at best is about 50 per cent at zenith. At the JCMT we use several different methods to estimate the extinction. The standard technique is to follow a bright source, typically a planet (for this purpose we also use Jupiter, Saturn and Venus) or a secondary calibrator, observe it with all filters for at least three different airmasses (preferably five or more), and make a least-squares fit to

$$V_{\rm obs} = V_{\rm i} \times {\rm e}^{-\tau_\lambda A}, \qquad (1)$$

where $V_{\rm obs}$ is the observed signal, $V_{\rm i}$ is the intrinsic signal, i.e. the signal one would measure above the atmosphere, τ_λ is the optical depth at the zenith at the wavelength λ and A is the airmass. This assumes that the sky stays constant during the observations, which is seldom the case. During changing sky conditions, one may get a perfectly good, but incorrect, fit to equation (1). Additional constraints are therefore needed. A quick check to assess whether the results are plausible is to derive the responsivities, i.e. the conversion factors, C_λ, from instrumental units (mV) to Jy beam^{-1}. At the JCMT we keep a record of these conversion factors for all filters, and, even though they vary as a function of water vapour (especially for the broad filters), they provide a first indication that the derived optical depths may be incorrect. For runs that span several nights, one can typically derive a more accurate calibration, especially if the PWV level stays about the same, since one can iteratively derive a solution of responsivities that work for the whole data set (cf. Sandell 1988).

Currently we have access to the sky monitor at 225 GHz on CSO (commonly known as CSO tau, see e.g. Masson 1993). The CSO radiometer does a sky dip every 10 min and hence we have a record of the 1.3-mm optical depth throughout the night. This has simplified the calibration of UKT14, because we can identify periods when the opacity has stayed constant. We have also determined linear relations between the optical depth in the UKT14 filters as a function of CSO tau. For most of the filters we can simply write

$$\tau_{\rm UKT14}(\lambda) = k_\lambda \times (\tau_{\rm CSO} - 0.01), \qquad (2)$$

where k_λ is a constant and 0.01 is the oxygen contribution to the $\tau_{\rm CSO}$ opacity (the rest of the optical depth is from the PWV in the atmosphere). For some of the broad filters (especially the 800-μm filter, which covers two atmospheric windows), k_λ is found to be a relatively strong function of PWV, and we are currently working on improving k_{800} as a function of PWV, see e.g. Stevens & Robson (1994) for recent least-squares fits to CSO tau. Another often-used method, especially when CSO tau is not available, is to look at the ratio of the derived optical depths at two wavelengths,

Table 2. Photometry of secondary calibrator sources. The numbers in parentheses denote the number of independent observations obtained for each source and filter/aperture combination (800-μm photometry is also given in the diffraction-limited aperture, i.e. HPBW = 13.5 arcsec), while a ... entry means that no observations were obtained. Errors are one standard deviation from the mean. All fluxes are given in Jy beam^{-1}.

FILTER HPBW	2mm 27″	1.3mm 19″	1.1mm 18.5″	850 μm 17.5″	800 μm 16.5″	800 μm 13.5″	750 μm 17.5″	450 μm 18.5″	350 μm 19.5″
SOURCE				ULTRACOMPACT HII REGIONS					
W3(OH)	5.5±0.3 (17)	10.2±0.5 (16)	12.8±0.3 (23)	25.5±0.5 (5)	30.9±1.3 (24)	26.5±1.4 (8)	39.9±0.9 (7)	222±16 (19)	498±64 (12)
G343.0	2.0±0.3 (2)	6.2±0.2 (2)	8.7±0.3 (9)	19.8±1.3 (2)	27.3±0.4 (7)	23.2±0.3 (2)	37.1±1.6 (3)	215±5 (5)	419±19 (3)
NGC 6334I	8.8±0.5 (17)	21.9±1.0 (23)	30.0±0.8 (22)	65.3±1.9 (10)	80.8±3.4 (20)	71.7±2.7 (7)	109.1±2.3 (2)	600±40 (9)	1263±139 (7)
G5.89	9.5±0.3 (14)	13.8±0.6 (17)	16.3±0.4 (22)	32.6±1.9 (7)	36.2±1.3 (16)	32.0±0.8 (11)	45.1±0.6 (2)	259±18 (8)	571±34 (10)
G10.62	7.1±0.2 (12)	13.2±0.6 (11)	17.2±0.5 (14)	37.0±1.2 (8)	43.7±4.1 (9)	38.1±2.1 (2)	...	356±20 (3)	788±82 (2)
G34.3	12.5±0.4 (7)	24.2±0.6 (8)	31.3±0.8 (24)	62.5±11.0 (2)	73.9±3.1 (17)	63.4±1.8 (7)	103.1±6.2 (3)	511±28 (13)	1125±80 (4)
G45.1	1.8±0.2 (4)	3.2±0.1 (8)	4.0±0.1 (8)	...	10.3±0.5 (7)	...	13.2±1.0 (3)	78±4 (3)	187±11 (3)
K3-50	6.5±0.2 (9)	8.5±0.4 (10)	9.2±0.3 (14)	15.8±0.5 (6)	17.9±0.8 (6)	16.7±0.3 (2)	21.9±1.8 (1)	110±13 (12)	241±16 (7)
ON-1	1.6±0.2 (3)	3.6±0.1 (4)	4.7±0.2 (4)	10.8±1.1 (3)	15.4±1.0 (3)	12.5±0.1 (1)	...	143±1 (1)	271±4 (1)
W75N	2.9±0.2 (13)	8.5±0.3 (22)	11.6±0.3 (22)	27.3±1.9 (22)	33.2±2.2 (23)	27.9±1.9 (7)	44.6±1.7 (9)	283±30 (15)	672±60 (9)
NGC 7538IRS1 IRS1	4.9±0.2 (7)	8.2±0.4 (10)	9.9±0.3 (12)	19.0±0.5 (7)	22.2±0.8 (11)	18.3±0.9 (8)	27.8±0.5 (1)	157±11 (11)	301±43 (11)
				LOW LUMINOSITY PROTOSTELLAR SOURCES					
GL 490	0.9±0.1 (7)	2.3±0.1 (7)	2.9±0.2 (16)	5.9±0.1 (3)	6.7±0.3 (8)	6.2±0.3 (5)	8.2±0.1 (1)	38±5 (5)	45±5 (2)
L1551-IRS5	0.7±0.2 (9)	1.7±0.1 (12)	2.4±0.1 (14)	...	6.2±0.3 (13)	5.7±0.3 (12)	8.2±0.5 (8)	41±4 (4)	95±5 (2)
NGC 2071IR	1.5±0.2 (6)	4.2±0.3 (5)	4.8±0.3 (8)	11.2±0.6 (5)	12.4±0.6 (6)	10.4±0.3 (6)	...	79±10 (6)	177±10 (5)
16293-2422	2.4±0.2 (13)	6.1±0.2 (18)	8.4±0.3 (38)	17.3±0.9 (8)	21.1±0.5 (34)	18.5±0.6 (26)	28.1±1.5 (7)	119±11 (16)	235±19 (14)
				STARS (AGB STARS, PLANETARIES AND PROTOPLANETARIES)					
CRL 618[a]	1.7±0.1 (10)	2.3±0.1 (11)	2.6±0.1 (13)	4.7±0.3 (1)	4.3±0.2 (16)	4.2±0.2 (9)	4.2±0.3 (9)	13±2 (14)	25±2 (10)
VY CMa	0.35±0.08 (3)	0.66±0.12 (3)	0.90±0.05 (4)	2.2±0.1 (1)	2.2±0.1 (6)	...	2.1±0.2 (2)	9.7±0.3 (3)	19±6 (3)
OH231.8+4.2	0.2±0.1 (3)	0.8±0.1 (2)	1.2±0.1 (3)	2.2±0.1 (1)	2.6±0.2 (5)	...	3.0±0.2 (2)	13±2 (3)	20±5 (1)
IRC+10216[b] $\phi = 0$	1.0±0.1 (2)	2.3±0.1 (3)	2.7±0.1 (5)	6.5±0.1 (1)	5.9±0.4 (3)	5.4±0.2 (3)	...	19±3 (3)	30±2 (1)
IRC+10216 $\phi = 0.6$	0.6±0.2 (2)	1.7±0.1 (2)	1.9±0.1 (4)	4.9±0.4 (4)	4.5±0.3 (5)	4.0±0.1 (1)	...	16±4 (3)	...
CRL 2688	0.7±0.1 (6)	2.1±0.1 (7)	2.7±0.1 (11)	5.6±0.1 (2)	6.5±0.2 (6)	...	7.0±0.6 (3)	24±3 (8)	46±5 (8)
NGC 7027	4.4±0.1 (10)	3.8±0.1 (2)	3.7±0.2 (15)	...	4.8±0.5 (15)	...	...	7.1±0.6 (5)	13±1 (1)

[a]The free-free emission from CRL618 has been steadily increasing (see text), resulting in an increase in flux for the 2 mm–800 μm bands. The flux densities for these bands are average of 1991 observations only.
[b]The flux densities for IRC + 10216 are given for the maximum ($\phi = 0$) at JD-244 7453 and for the following minimum, which occurs at $\phi \simeq 0.6$.

most commonly the ratio τ_{800}/τ_{1100}. Under dry sky conditions this ratio is expected to be ~4, and in wet conditions it may approach 3 (again the spread in this ratio reflects the change in the effective filter bandpass as a function of PWV). The ratio method is similar to deriving responsivities, but, since the responsivities of the 1100- and 800-μm filters change in the same direction, it is less sensitive to the PWV content in the atmosphere.

During wet nights we expect to observe lower fluxes for a secondary calibrator, especially at 2 mm and 800 μm, due to the changes in effective frequency of the filter towards longer wavelengths (Duncan et al. 1990). We have carried out tests on G10.62 and NGC 6334I to quantify how much this will affect the data at 800 μm. We used observations from several wet nights and calibrated the data by recomputing planetary fluxes for the effective wavelength derived from the estimated PWV (4–5 mm). We found that the 800-μm flux was about 10 per cent lower than an average of all the dry nights. The data in Table 2 are total averages of all data, but the bulk of the data originates from relatively dry nights.

After all the data have been calibrated, we have normally formed one-night averages, although in some cases the data may have been taken as separate observations. Data from single nights have been treated as independent observations only if they are calibrated against another standard or if they were taken several hours apart. The majority of the data, however, come from data sets obtained during different nights. After all the data have been collated, we compute unweighted means, i.e. all the data points have the same weight regardless of their formal errors. The standard deviation of the mean gives a good measure of the systematic errors in the calibration, which is the dominant error at submillimetre wavelengths. For small data sets it may be misleading because most of the data may come from an extended run and have similiar systematic errors. In this case the standard errors may underestimate the true uncertainty of the flux densities. For data sets that have more than 10 data points, most of the 1100-μm data have errors ≤5 per cent, most of the 800-μm data have ~10 per cent errors, and most of the 450- and 350-μm data have errors of 10–15 per cent, and seldom more than 20 per cent.

4 DISCUSSION

All the sources listed as secondary calibrators in this paper have usually been observed with a 60-arcsec azimuth chop, although all UCHII regions have also been observed with a 150-arscec azimuth chop. Within the accuracy that one can normally achieve in the submillimetre regime, we have found no measurable difference in the observed fluxes. Chop throws of <60 arcsec should be avoided for all UCHII regions and protostellar sources, and for IRC + 10216, while the AGB stars have been observed with chops down to 40 arcsec without any detectable change in the flux density (see e.g. Knapp et al. 1993). We now briefly discuss the different categories of secondary calibrators and comment on a few of the objects.

4.1 UCHII regions and protostellar sources

All of the low-mass protostars, and especially some of the UCHII regions, are very bright. This means that they can be used as flux standards, especially at submillimetre wavelengths, during all acceptable weather conditions. All sources of this class are typically characterized by a compact bright core surrounded by fainter extended emission, which may occasionally extend out to more than 60 arcsec. They may still be usable as calibrators, nevertheless, if the extended emission is relatively uniform or if the emission is completely dominated by the core, i.e. the extended emission is no more a few per cent of the core emission. All sources in these categories, which we have adopted as standards, are associated with some extended emission, but all of them still appear to be good calibrators. Almost all UCHII regions show secondary components within the core regions, especially when mapped at high resolution at 450 μm. This will clearly create problems if the calibrators are observed with HPBW≤10 arcsec. In our sample, the only two sources that appear single at 450 μm are NGC 6334I and K3-50, but we note that we have not obtained 450-μm maps of G343.0, G45.1 or ON-1, and that 800-μm maps of these sources show only a single source, suggesting that they may all be isolated.

4.1.1 *W3(OH)*

This strong UCHII region exhibits some faint extended emission at radii ≥60 arcsec in a ridge to the north-east (position angle ~70°). The emission is about 1–2 per cent of the peak emission, and does not show up in our photometry. At 450 μm the core emission is resolved into two sources separated by ~10 arcsec.

4.1.2 *NGC 6334I*

This is the northernmost UCHII region in the large high-mass star formation region NGC 6334, which was first mapped at 1.0 mm by Cheung et al. (1978). Their map, which had a resolution of 1 arcmin, showed extensive emission over the whole cloud complex with the strongest emission peaking on NGC 6334I. The NGC 6334I and I(N) region (Gezari 1982) has since been extensively mapped in the (sub)millimetre by Sandell & Baas (in preparation). The molecular cloud still extends further north with a number of embedded young objects. Some of these objects, such as NGC 6334I(N), are strong in the (sub)millimetre but are not suitable as calibrators, because they are surrounded by extended strong dust emission. Although NGC 6334I is associated with some extended emission both to the north and to the north-west, this is completely dominated by the strong emission from the core and does not affect the quality of our photometry.

4.1.3 *NGC 7538 IRS1*

The molecular cloud associated with NGC 7538 appears to host a cluster of very young high-mass stars. The first 1-mm map of this region (Werner et al. 1979) did not resolve any individual sources, although it showed the dust emission to peak in the vicinity of IRS1. High-resolution mapping with JCMT in the (sub)millimetre (Sandell & Baas, in preparation) shows that there are four major submillimetre sources in this deeply embedded cluster, namely IRS1, the H_2O maser ~100 arcsec south of IRS1 (occasionally mislabelled as IRS11), and the two sources associated with IRS9a,b. The (sub)millimetre maps reveal a clear bridge of emission to the H_2O maser to the south, and also strong emission to both the north-west and the south-east (i.e. toward IRS9). The dust emission from IRS1 is extended in the whole (sub)millimetre regime, and becomes even more extended and lumpy at 450 and 350 μm because some of the components of this source complex have steep spectra. Although the photometry of IRS1 quoted in Table 2 appears to be sound, the data should be treated with caution, because the mapping indicates that the photometry could be affected by the extended emission.

4.1.4 K3-50

This source is also part of a star formation cluster, and one can see faint emission in the direction of ON-3, i.e. at a position angle of ~45°. The emission of the K3-50 core is strong, and our photometry has revealed no dependence on the position angle of the chop within observational errors.

4.1.5 L1551 IRS5 and NGC 2071IR

These sources are both associated with extended faint emission, but, with the photometric accuracy achieved on these objects, we see no difference between, say, a 60-arcsec and a 150-arcsec chop. Deep 800- and 450-μm maps of NGC 2071IR (Sandell, Robson & Walther, in preparation) show that the strongest emission extends towards the north-west in a position angle of ~ −30°. Unless the source is observed at low elevations close to setting, one should generally not chop on to this faint ridge (which has a flux density at 800 μm of ≤0.5 Jy beam^{-1} ~60 arcsec from the centre). At short wavelengths, the emission from NGC 2071IRS is resolved into three sources (IRS1, 2 and 3, all within 10 arcsec), which would cause problems if photometry were performed with beamsizes ≤10 arcsec.

4.1.6 16293−2422

At 3 mm this is a binary system (Mundy et al. 1992). Careful mapping at JCMT (Sandell, in preparation) shows that for wavelengths shorter than 1.1 mm the southern source, MM1, completely dominates the dust emission. Deep 800-μm maps reveal some faint extended emission, but this is only at the 1–2 per cent level at a radius of 60 arcsec from the core. Larger chop throws should be avoided, because the cold DCO^+ region 80 arcsec east and 22 arcsec south of 16293 is associated with significant continuum emission. 16293 has been extensively observed in the (sub)millimetre and, since it is strong and compact, it is possibly one of the best calibrators we have for wavelengths shorter than 1.3 mm.

4.2 Protoplanetaries and AGB stars

4.2.1 IRC+10216

As already mentioned, IRC+10216 is by no means an ideal calibrator, because it has long-period variations in the whole (sub)millimetre regime. At 1.1 mm we have obtained a relatively well-sampled 'light curve' over two periods (Fig. 1). The period is well determined as 635 d, and the maximum flux, based on optical and near-IR data (Alsknis 1989), occurs at

$$\mathrm{JD} = 244\,1738 + 635\,\mathrm{d} \times E. \quad (3)$$

Alsknis (1989), however, notes that IRC+10216 has a long-term secondary variation of ~15 yr, and that the luminosity again appears to have reached a high state. Recent, although sparsely sampled, JCMT observations indicate that the (sub)millimetre fluxes may now be higher than those presented in Table 1 (Knapp et al., in preparation).

4.2.2 VY CMa and OH231.8

Both VY CMa and OH231.8 are long-period variables, and the submillimetre flux densities may vary by about 20 per cent (see e.g. Knapp et al. 1993). This level of variability is difficult to see in the unevenly sampled data we have on these two stars, and therefore the values given in Table 2 refer to total averages of all data, which cover less than one stellar period.

4.2.3 CRL618

The flux density of CRL618 appears to be slowly rising at wavelengths where the free–free emission is dominating or significant, i.e. at wavelengths from 2 mm to 800 μm (Knapp et al. 1993). No measurable change has been seen in the 450- and 350-μm bands where the flux density is completely dominated by the thermal dust emission from the circumstellar envelope. For this source we have therefore compiled an average of all observations at 450 and 350 μm, while the wavelength bands from 2 mm to 750 μm are one-year averages for 1991. We note that the flux density at these wavelengths is still likely to rise, and therefore CRL618 should be used with caution as a calibrator in this region.

ACKNOWLEDGMENTS

I especially thank E. I. Robson and W. D. Duncan, who were part of the team that made the first selection of potential submillimetre standards, and who have been very helpful in providing additional data during the years. C. Aspin and M. J. Griffin have provided many useful comments on the paper. I also acknowledge calibrated data obtained from D. Hughes, D. Weintraub, P. Friberg, M. J. Griffin, S. Skinner and C. Rogers. The James Clerk Maxwell Telescope is operated on a joint basis between the United Kingdom Particle Physics and Astronomy Research Council (PPARC), the Netherlands Organization for the Advancement of Pure Research (ZWO), the Canadian National Research Council (NRC) and the University of Hawaii (UH).

REFERENCES

Alsknis A., 1989, Inf. Bull. Variable Stars, 3315
Cheung L., Frogel J. A., Gezari D. Y., Hauser M. G., 1978, ApJ, 226, L149
Duncan W. D., Robson E. I., Ade P. A. R., Griffin M. J., Sandell G., 1990, MNRAS, 243, 126
Gezari D. Y., 1982, ApJ, 259, L29
Griffin M. J., Ade P. A. R., Orton G. S., Robson E.I., Gear W. K., Nolt I. G., Radostitz J. V., 1986, Icarus, 65, 244
Griffin M. J., Orton G. S., 1993, Icarus, 105, 537
Kieffer H. H., Martin T. Z., Peterfreund A. R., Jakosky B. M., Miner E. D., Don Paluconi F., 1977, J. Geophys. Res., 82, 4249
Knapp G. R., Sandell G., Robson E. I., 1993, ApJS, 88, 173
Masson C., 1993, in Ishiguro M., Welch W. J., eds, ASP Conf. Ser. Vol. 59, Astronomy with Millimeter and Submillimeter Wave Interferometry. Astron. Soc. Pac., San Francisco, p. 82
Mundy L. G., Wootten A., Wilking B. A., Blake G. A., Sargent A. I., 1992, ApJ, 385, 306
Orton G. S., Griffin M. K., Ade P. A. R., Nolt I. G., Radostitz J. V., Robson E. I., Gear W. K., 1986, Icarus, 67, 289
Sandell G., 1988, Note to UKT14 users, JCMT internal memo
Sandell G., 1989, Draft catalogue of secondary calibrators, JCMT internal publication
Stevens J. A., Robson E. I., 1994, MNRAS, submitted
Weintraub D. A., Sandell G., Duncan W. D., 1989, ApJ, 340, L69
Werner M. W., Becklin E. E., Gatley I., Matthews K., Neugebauer G., Wynn-Williams C. G., 1979, MNRAS, 188, 463
Wright M., Sandell G., Wilner D. J., Plambeck R. L., 1992, ApJ, 393, 225